

# Thermal performance enhancement of evacuated tube solar collector using MWCNT, Al<sub>2</sub>O<sub>3</sub>, and hybrid MWCNT/ Al<sub>2</sub>O<sub>3</sub>nanofluids

Engy Elshazly<sup>a,\*</sup>, Ahmed A. Abdel-Rehim<sup>a</sup>, Iman El-Mahallawi<sup>a,b</sup>

<sup>a</sup> The Centre for Renewable Energy, The British University in Egypt, Cairo 11837, Egypt

<sup>b</sup> Department of Metallurgical Engineering, Faculty of Engineering, Cairo University, Giza 12613, Egypt

## ARTICLE INFO

### Keywords:

Solar water heater  
Heat transfer fluid heat pipe  
Evacuated tube  
Thermal energy storage  
Heat transfer enhancement  
Nanofluids  
Energy efficiency

## ABSTRACT

Nanofluids have numerous applications in heat transference procedures due to their exceptional thermal characteristics. The most desirable parameter to enhance the solar collector's performance is the enhancement of the convective heat transfer coefficient between the working fluid tubes and the absorber. As a result, nanofluids have gained prominence as working fluids in solar thermal systems. The trendsetting review reveals that mostly the nanofluids in solar collectors are based on water employing nanoparticles of Al<sub>2</sub>O<sub>3</sub>, TiO<sub>2</sub>, SiO<sub>2</sub>, and CuO. Besides, nanoparticle concentration is a challenging factor in using nanofluids. In this research, under controlled conditions, the working fluids multi-wall carbon nanotube, Aluminum Oxide, and hybrid MWCNT/Al<sub>2</sub>O<sub>3</sub> 50:50% were experimentally examined for the thermal efficiency enhancement of the evacuated tube solar collector. For each type of nanofluid, four volume concentration percentages (0.5%, 0.025%, 0.01%, and 0.005%) were examined along with three distinct mass flow rates. According to the findings, using hybrid MWCNT/Al<sub>2</sub>O<sub>3</sub> 50:50% delivers an efficiency boost of about 20% overusing Al<sub>2</sub>O<sub>3</sub>, as was previously reported. Finally, it was found that the utilization of 0.5% MWCNT/water nanofluid at 3.5 L/m can enhance the ETSC's energy and exergy efficiency to reach 73.5% and 51% respectively while reaching approximately 60% and 44% for Al<sub>2</sub>O<sub>3</sub>, and 69% and 38% for hybrid MWCNT/Al<sub>2</sub>O<sub>3</sub> (50:50%) under the same test conditions.

## 1. Introduction

We are facing the challenges of decreasing fossil fuel availability. Many alternative renewable sources of energy could actively bring down the utilization of conventional fuel supplies. Solar energy is a crucial option in many developing countries' commercial and industrial sectors to narrow the use of fossil fuels and their harmful environmental impact. Solar water heating (SWH) is a cost-effective method of generating hot water for domestic or commercial process heating utilizing solar thermal energy. The solar heat collector should be opted for based on the amount of energy it takes, the desired thermal spectrum, as well as the system's economy. In hospitals, domestic uses, and other operations in several businesses, huge quantities of energy go sunk and wasted specifically for water heating. Water heating utilizes a huge amount of fossil fuel, resulting in environmental damage and climate change owing to greenhouse gas emissions. In general, a solar collector is regarded as thermal equipment because it is designed to capture solar energy and convert it to heat energy. These systems usually get benefited from utilizing the working fluid that acts as an energy carrier by traveling

through the solar collector pipes and absorbing the sun's energy. Although there are many different types of solar collectors, they can be mainly classified as stationery and sun-tracking concentration collectors. Stationary collectors consist of Evacuated Tube Solar Collectors, Flat Plate Solar Collectors, and Compound Parabolic [1].

Flat Plate Solar Collector (FPSC) and Evacuated Tube Solar Collector (ETSC) are the two most common types of solar water heaters. The ETSCs are characterized by vacuum insulation and careful exterior coating of the absorber component, resulting in high heat derivation functioning, heat loss can be decreased, and is suitable for foggy or severely cold circumstances. FPSC is a well-known solar collector for providing fluid temperatures in the 50–100 °C range, among other solar thermal collectors. Both forced; using a circulation pump, and thermosiphon water circulation; which uses the thermosiphon effect of water to operate, are used by SWH systems. Additionally, the working fluid is the component that absorbs the most heat from the collector, so replacing conventional fluids with nanofluids may be the most efficient technique to enhance heat transfer in the collectors under discussion [2]. Thermal energy is by far the most widely employed form of solar energy in water boiling and heater systems in both residential and commercial settings.

\* Corresponding author.

E-mail address: [engy.samy@bue.edu.eg](mailto:engy.samy@bue.edu.eg) (E. Elshazly).

<https://doi.org/10.1016/j.ijft.2022.100260>

Received 1 September 2022; Received in revised form 29 November 2022; Accepted 29 November 2022

Available online 1 December 2022

2666-2027/© 2022 The Author(s). Published by Elsevier Ltd. This is an open access article under the CC BY-NC-ND license (<http://creativecommons.org/licenses/by-nc-nd/4.0/>).

Nomenclature		Qu	Useful Energy Gain [W]
ETSC	Evacuated Tube Solar Collector	$S_{gen}$	Entropy generation
FPSC	Flate Plate Solar Collector	bf	Base fluid
MWCNT	Multi-wall carbon nanotubes	nf	Nano Fluid
$Al_2O_3$	Aluminum oxide	np	Nanoparticle
T	Temperature	<i>Greek Symbols</i>	
$T_{in}$	Inlet temperature	$\varphi$	Nanofluid volume Concentration
$T_{out}$	Outlet temperature	$C_p$	specific heat capacity [J/kgK]
TEM	Transmission electron microscopy	k	thermal conductivity [W/mK]
SEM	Scanning Electron Microscopy	$\rho$	Density [ $kg/m^3$ ]
TGA	Thermogravimetric analysis	$\eta$	Efficiency
$F_R$	Heat removal factor	$\eta_{ex}$	Exergy
G	Radiation intensity [ $W/m^2$ ]	$\tau$	Transmissivity
Ac	Collector area [ $m^2$ ]	$\varepsilon$	Emissivity
$\dot{m}$	Mass flow rate [kg/s]	$\alpha$	Absorptivity

Due to its simple operating principle, solar water heating is the most common application of solar energy around the world [3].

According to Perea-Moreno et al., solar thermal systems might cut annual emissions by 90  $\alpha$ .14 tons of  $N_2O$ , 804.2 tons of  $CO_2$ , and 0.114 tons of  $CH_4$ . The energy-conversion efficiency of solar collectors is low, and research has been done to enhance it. To address this issue, numerous studies on the application of various working fluids have been carried out. It is a common method to change the working fluid to increase the solar collector's efficiency by adding high thermal conductivity nanoparticles. A nanofluid is a fluid that contains a relatively small quantity of uniformly distributed and suspended nano-sized particles with an average size of fewer than 100 nanometers in the base fluid. When a little percentage of nano-sized particles is added to a pure fluid, its thermal conductivity is increased, and the fluid is called nanofluid. Nanofluid has gained popularity in scientific research in the field of heat transfer in recent years, notably for renewable energy applications. Solar collector efficiency is improved by using nanofluids. As a result, more heat from the sun is received, and the demand for fossil fuels is reduced. If nanoparticles are uniformly disseminated and stably floating in base fluids, their partial contribution improves the thermal characteristics of the base fluid [4].

Nanofluid was first invented by Choi in 1995, with nano-sized particles varying from 1 to 100 nm in colloidal amalgam accompanying the working fluid and the nanoparticle fluid mixtures. Nanoparticles are made from a variety of materials, which includes both carbide and oxide ceramics, metals, nitrides, semiconductors, nanotubes made of carbon, and other composite materials including nanoparticle & core-polymer composites and alloyed nanoparticles depending on the application [5]. "Hybrid metals" are created when two or more materials are blended in such a way that the resulting blend would have an entirely new chemical bond. In fact, "hybrid nanofluid" was coined when more than one metal derived a homogenous phase with concurrent mixing. When compared to unitary nanofluids, such a modern class of nanofluids demonstrated potential improvements in heat transport characteristics as well as thermophysical and hydrodynamic characteristics [6]. Aside from the nonmetal components, the metal and other materials used for the nanoparticles, and different structures that have been used, are referred to as "doped" with molecules in the solid-liquid state. The result is the acquisition of exceptional thermal properties associated with the smallest practicable volume fraction ( $\Lambda = 1\%$ ). As a result, improved heat transfer requires floating nearly mono-dispersed nanoparticles or non-accumulated in mixtures [7]. When utilizing a 1% nanoparticle concentration, the heat enhancement of a nanofluid flow over water flow is around 5%, and it rises to 12% when using a 2% nanoparticle concentration [8].

The main four primary benefits of utilizing nanofluids in solar

**Table 1**

Thermal conductivity (k) of different metal oxides values at 300 K. [11].

Material	k
$SiO_2$ , polycrystalline	1.38
$TiO_2$ , polycrystalline	8.4
$Al_2O_3$ , polycrystalline	36
$Al_2O_3$ , Sapphire	46

thermal systems can be stated as follows. First, nanofluids have high conductivity, and heat transmission coefficient, also the reduced specific heat of such particles, increases the efficiency of thermo-devices. Second, nanoparticles possess a very reduced size and a big surface area, which results in an exponential rise in the heat valence of nanofluid and solar energy absorption. Third, better optical properties; better optical properties include greater absorption and extinction coefficients. Fourth, nanofluids take out the needed heat transmission area and lower the important transmission surface in these systems. Fifth, the advantages of nanofluids over micro-suspension; nanofluids have higher stability in terms of clogging and sedimentation of pumps and pipes due to their extremely small size when compared to micro or suspended mill-sized particles, and that is an important aspect to be considered in several solar applications [9].

One of the most difficult aspects of employing nanofluids is the increase in pressure drop and pumping power caused by high viscosity and nanoparticle concentration. MWCNT and  $Al_2O_3$  have been the most common nanofluids, with a few additional nanofluids such as CuO, ZnO, SWCNT, Ag,  $SiO_2$ ,  $Fe_2O_3$ , and  $TiO_2$  [10]. Table 1 gives the readings of different metal oxides that are generally employed as heat transfer materials at 300 K temperatures.

The ETSCs have been investigated using nanofluids in many experimental and numerical studies. High-concentrated SWCNT nanofluids have better thermal conductivity, allowing more heat to be absorbed by the fluid. The Brownian flow had a significant impact on the evacuated collector system due to the circulation of nanofluid in the tube at a particular flow rate rather than being stopped. The thermal performance was compared to the state with water, it was discovered that employing SWCNT nanofluids as heat transfer fluid increased collector efficiency. More specifically, the comparable maximum efficiency in this circumstance was 0.2 vol%. At a mass flow rate of 0.025 kg/s, the efficiency of SWCNT nanofluids was discovered to be 93.43% and 48.57% for 0.05 vol% nanoparticle concentration. By increasing the volume percentage of SWCNT nanoparticles and increasing the mass flow rate, the collector efficiency improved [12]. Another experimental study by Mahbulul

et al., revealed that the ETSC's efficiency can be enhanced by 10% by applying 0.2 vol.% of SWCNT compared to water under the same experimental conditions [13].

In an experimental investigation of the use of MWCNTs as a working fluid in a solar plate collector, Natarajan and Kiatsiriroat discovered that MWCNTs significantly outperform most other nanoparticles, especially for high temperatures applications [14]. According to Faizal et al., lowering the collector size by 37% can be employed by using MWCNT/water as the working fluid while keeping the same efficiency [15]. Tong et al., studied the effect of using MWCNT/water as a base fluid for ETSCs. The results show that by using MWCNT/water with a concentration of 1% as a working fluid, the ETSC's efficiency increased by 8% compared to water [16]. A theoretical study done by Kim et al. shows that applying MWCNT/water with 0.2 vol.% in U-tube ETSC can improve its efficiency to reach 62.8% [17].

Dehaj et al. used MgO nanofluid to perform an experimental analysis based on an ETSC. Water/magnesium oxide nanofluids with concentrations of 0.014 percent and 0.032 percent were combined and tested in a heat pipe ETSC at flow rates of 5, 8, 11, and 14 L/min. It was discovered that the heat pipes ETSC using the considered nanofluid have substantially greater efficiency of 69% and 77% for the two studied flow rates respectively compared to 60% for using base water. Furthermore, the ETSC's thermal performance is influenced by the flow rate and working fluid [18].

Because of their high thermos-physical properties, TiO<sub>2</sub> nanofluids outperformed water in terms of yield. ETSC thermal performance was enhanced by 42.5% by employing TiO<sub>2</sub>/water with a concentration of 2% as proved by Mahendran et al. [19]. Farajollahi et al. tested various nanofluids in a heat exchanger to find the most effective nanofluid in a turbulent flow. In comparison to their contemporaries, the experimental results show that TiO<sub>2</sub> is more effective. Al<sub>2</sub>O<sub>3</sub> outperformed TiO<sub>2</sub> in higher concentrations of nanofluid [20]. Mirzaei et al. found that at the ideal flow rate of 2 L/m, the use of Al<sub>2</sub>O<sub>3</sub> nanocomposites with a volumetric concentration of 0.1 percent boosted the collectible efficiency by 23.6 percent [21]. Rajput et al. found that raising the Al<sub>2</sub>O<sub>3</sub> nanofluid concentration from 0.1 percent to 0.3% boosted effectiveness by 21.32% [22]. Ghaderian and Sidik's experimental investigation of using Al<sub>2</sub>O<sub>3</sub>/water nanofluid with 0.06% concentration shows that the system's efficiency can increase by 36% and reach a maximum value of 58.65% [23].

Hybrid nanofluid and thermal technologies are critical for energy exchange and solar sensor performance improvements. The temperature conductance of hybrid nanofluids may be affected by the concentrations or solid volume proportion of nanoparticles, which is directly linked to the nanoparticle dimension as well as the volume circulation channel of fluid [24].

To validate the manufactured nanocomposites, the hybridized fluids

created by the dissemination of different materials in working fluids need to be characterized, where the greater the fluid nanoparticles content, the greater the viscosity, and the lower the mass flow rate will be. An experimental investigation was performed for rheological properties prediction of MWCNTs–ZnO/water– Ethylene glycol (80:20 vol. %) hybrid non-Newtonian nanofluid with volume fractions of 0.075%, 0.15%, 0.3%, 0.6%, 0.9%, and 1.2% in the temperature range of 25–50 °C. The results show that by increasing the nanoparticle's volume fractions, its effect is better, and the non-Newtonian property is more likely to appear. On the other hand, the fluid's viscosity is reduced by 21%, 17%, and 8% percent, respectively, at 50 °C, 40 °C, and 30 °C for the maximum volume fraction [25].

Heat transfer and mixing quality of a hybrid nanofluid containing silver Ag and iron oxide Fe<sub>3</sub>O<sub>4</sub> nanoparticles on distilled water inserted in a microchannel equipped with a dual mixer in different volume fractions were assessed. It was concluded that both the volume fraction and the Reynolds number have positively influenced heat transfer. However, the volume fraction has a bigger impact on boosting heat transfer than velocity. In addition, the mixing quality may improve or deteriorate with time for high Reynolds numbers and a steady frequency. While the mixing quality rapidly improves over time at low Reynolds numbers, it takes at least 0.015 s to reach stable heat transmission [26].

The effect of temperature and volume fraction on the viscosity of a hybrid nanofluid ZnO/Ag 50:50%/Water was experimentally evaluated. Results indicate that the dynamic viscosity increases with increasing nanoparticle volume percentage and decreases with increasing temperature. While a rise in relative viscosity is connected to a rise in volume fraction at all temperatures [27].

According to Harandi & Karimipour, whenever a hybrid nanofluid is made employing Al<sub>2</sub>O<sub>3</sub>/Fe, Al<sub>2</sub>O<sub>3</sub>/water, with a concentration of 0.05 and 0.2%wt., the volume percentage increases the effectiveness of heat exchange by 6.9% [28]. Eidan et al., employed Al<sub>2</sub>O<sub>3</sub>/CuO acetone nanofluids in their study, with each studied condition efficiency being compared to acetone-based fluid. Experiments were performed with two volume concentration values (0.025% and 0.05%) and the enhancement percentage reached maximum of about 34%, 74%, 32%, and 73%, respectively [29].

Using MgO/MWCNT (50:50) hybrid nanofluid produced the highest thermal performance compared to MgO/MWCNT 90%:10%, MgO/MWCNT 80%:20%, MgO/MWCNT 70%:30%, and MgO/MWCNT 60%:40%, hybrid nanofluids at all studied flow rates, but it was marginally lower than MWCNT/water nanofluid based on Shady et al. research [30].

As observed from the literature review that the working fluid in a solar collector act as a heat transfer medium and a thermal energy absorber, when nanofluids are used as the working fluid, the



Fig. 1. ETSC complete system.

**Table 2**  
ETSC specifications.

Parameter	Value
ETSC Gross Area	2.35 m <sup>2</sup>
ETSC Active Area	1.407 m <sup>2</sup>
Number of Tubes	15
Tube Length	180 cm
Glass Transmissivity	$\tau \geq 92\%$
Absorber Emissivity	$\epsilon \leq 8\%$
Absorber Coating Emissivity	$\epsilon \leq 5\%$
Absorber Absorptivity	$\alpha \geq 92\%$
Absorber Plate Material	Aluminum
Cycle's Working Fluid volume	3.46 L
Collector's Working Fluid space capacity	1.256 L
Heat Pipe Material	High purity copper

performance of the solar collector can change, potentially leading to higher efficiencies. The most noticeable effect of employing nanofluids in solar collectors is an increase in thermal absorption and heat transfer rate depending on the nanoparticle type added.

Investigations into the impact of hybrid nanofluids on solar collectors have been ongoing for a while. The family of carbon-based nanotubes, which is the highest conducting nanoparticle used in solar collector applications, was depicted in the literature. On the other hand, the aluminum oxide was observed to have a great enhancement in solar collectors' efficiency while having lower cost and environmental impacts. However, it was shown that carbon nanotubes, aluminum oxide, and hybrid combinations need a more extensive experimental study to explore the response of ETSC in terms of energy, exergy, total heat gained, the enhancement in the collector's area to provide the same thermal energy, and the efficiency improvement toward using MWCNT, Al<sub>2</sub>O<sub>3</sub> and hybrid MWCNT/Al<sub>2</sub>O<sub>3</sub> at the same working conditions for higher concentrations and mass flux rates which will be explored in this study.

The main goal of this study is to engage the MWCNT – Al<sub>2</sub>O<sub>3</sub>/water nanofluids in the ETSCs to show the improved natural convection performance and to compete and access the performance of ETSCs including the MWCNTs, Al<sub>2</sub>O<sub>3</sub>, and hybrid MWCNT/ Al<sub>2</sub>O<sub>3</sub> 50%:50% at various flow rates in thermal energy, system efficiency, and exergy. The study also indicates the reduction percentage in the collector's area when using different nanofluids compared to water.

## 2. Experimental method

### 2.1. Experimental study

The purpose of the research's initial phase is to examine the energy use and associated efficiency of a heat pipe ETSC utilizing varied composition partakes of MWCNT/Water nanofluid at various rates of flux varying from 1.5 L/m to 3.5 L/m. Second, utilizing varying compositions of Al<sub>2</sub>O<sub>3</sub>/Water nanofluid at various rates of flux rates fluctuating from 1.5 to 3.5 L/min, and finally, employing varied compositions of hybrid MWCNT- Al<sub>2</sub>O<sub>3</sub>/Water nanofluid again at different rates of flow of 1.5, 2.5 and 3.5 L/min. As represented in Fig. 1, this experiment work is performed on an educational system, the ETSC with a 1.407 m<sup>2</sup> aperture area and 15 evacuation tubules. The evacuation tubes are 1.8 m long and have an inner diameter of 47 mm and an outside diameter of 58 mm; every tube has a heating pipe within the middle of the assembly, which is surrounded by an aluminum fin to maximize the absorption area. The heat pipes are filled with thermally conductive liquid and attached to the manifold. In comparison to an air-filled compartment, a vacuum fills the gap between the employed tubes and the exterior cover, minimizing conduction heat losses. With a 210 L tank capacity, a heat exchanger provides a closed loop for the fluid. Solar collector specifications are shown in Table 2.

The system comprises four thermocouple sensors of type PT1000, with a range of -40 to 150 °Celsius, and a screen to show the readout. Thermocouples are utilized to monitor the temperature of the collector as well as the inlet and outlet of the tank. The YF-S201 flow meter is used to observe the fluid's flow.

In the experiment, an artificial sunlight system was employed to reproduce sun radiation inside the laboratory. To manage the system's radiation output level, a radiation sensor, type 21 R7s 500-Watt, was linked to the lights. A PYR 1307 sun power meter sensor and a solar pump station were used to detect solar intensity (UniMaxx-Plus-SC-500-AC-V3). A monitoring and control system is included in the system with a 210 Liter tank where the used fluid is circulated in a closed loop connected to a heat exchanger connected to the collector. The ETSC is illustrated in Fig. 2.

In this research, the distilled water results served as the comparison's reference values. the experiment then employed four different concentrations of nanofluids in the tests: 0.005%, 0.01%, 0.025%, and 0.05%

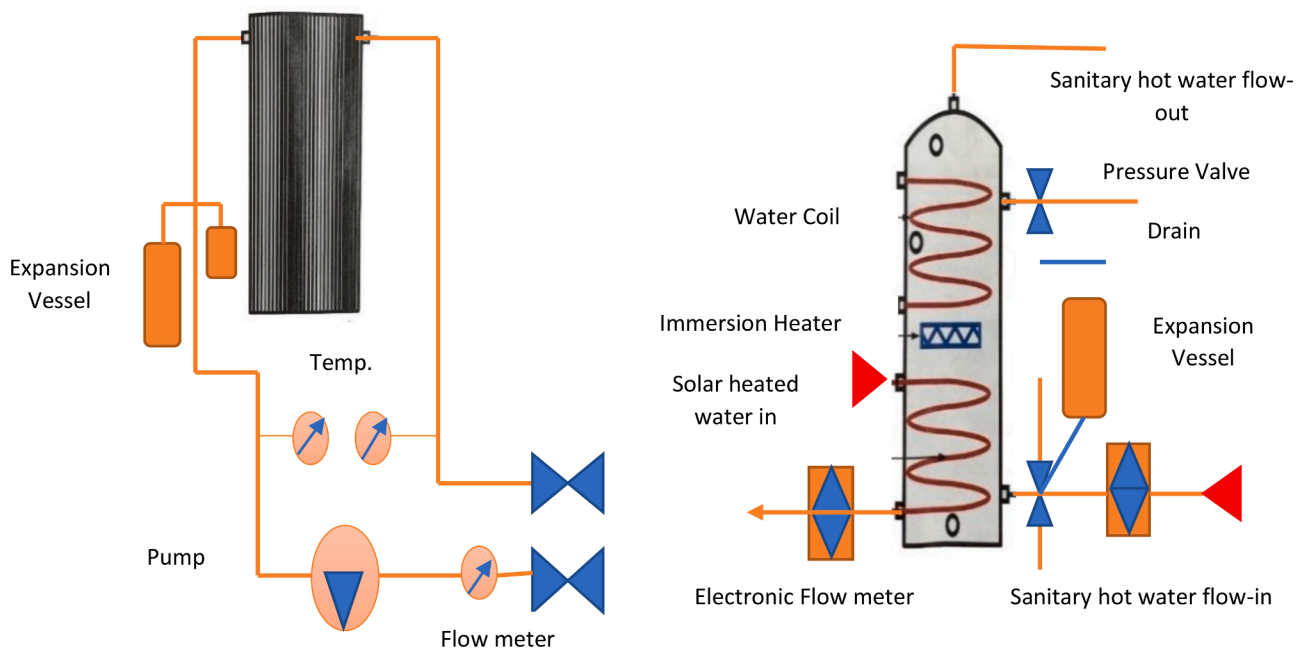


**Fig. 2.** Complete system diagram.



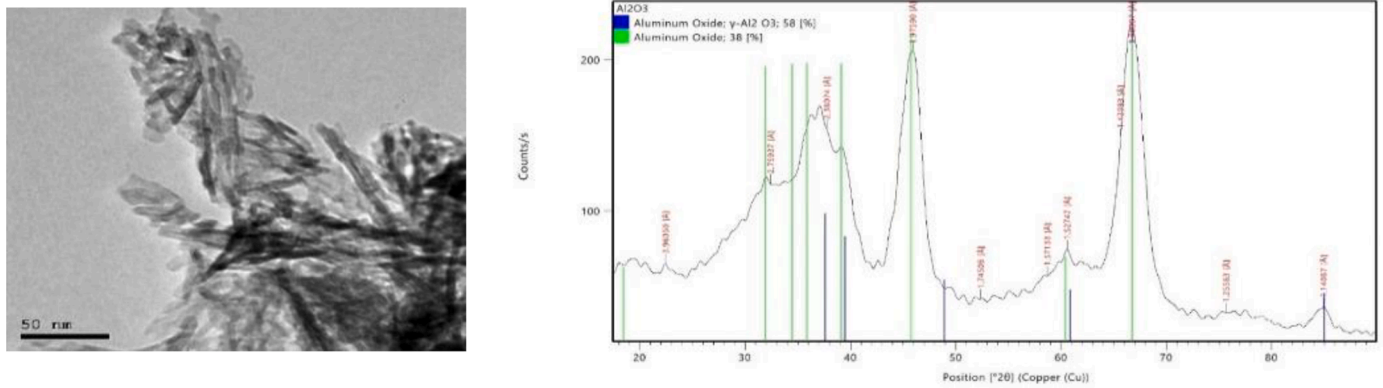


Fig. 3. TEM images and XRD pattern of Alumina nanoparticles.

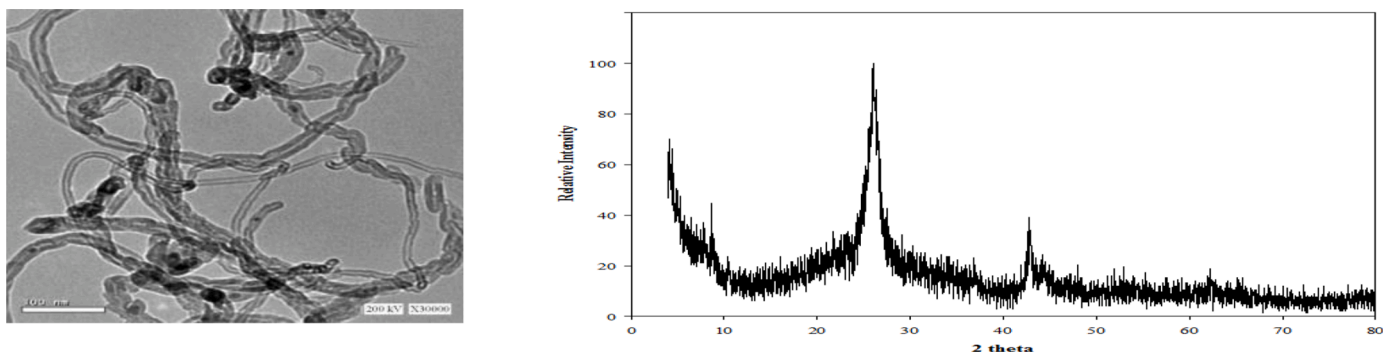


Fig. 4. TEM images and XRD pattern of MWCNT nanoparticles.

**Table 3**  
TEM properties of Al<sub>2</sub>O<sub>3</sub> nanoparticle.

Color	White.
Form	powder.
Average Size	< 30 nm
Shape	Spherical

**Table 4**  
TEM properties of MWCNT nanoparticle.

Parameter	Value	Test Method
Diameter	10–40 nm	TEM
Length	Up to 5 μm	SEM
Purity	>90%	TGA

by weight fraction for three flow rate values; 1.5, 2.5, and 3.5 L/m.

### 2.2. Nanofluid preparation

The creation of nanofluids is a crucial step in using nanoparticles to improve fluid thermal conductivity. The single-step technique and the two-step technique are the two most prevalent methods for producing nanofluids. To provide excellent thermal characteristics for nanofluids, it is critical to producing stable and robust nanofluids [31]. For this experiment, the two-step approach was applied due to its greater stability and durability. Distilled water was utilized to be the base fluid. The working fluids were Al<sub>2</sub>O<sub>3</sub> nanofluids with four concentrations of 0.005%, 0.01%, 0.025%, and 0.05% by weight fraction. Sol-gel, controlled boehmite precipitations, and hydrothermal processing are all used in the synthesis of Al<sub>2</sub>O<sub>3</sub> nanoparticles. Alkoxides, metallic powder, and aluminum salts are typically used to make boehmite. A sol-gel approach using an aluminum nitrate precursor and an ammonium carbonate pathway with spherical nano-sized particles was used to

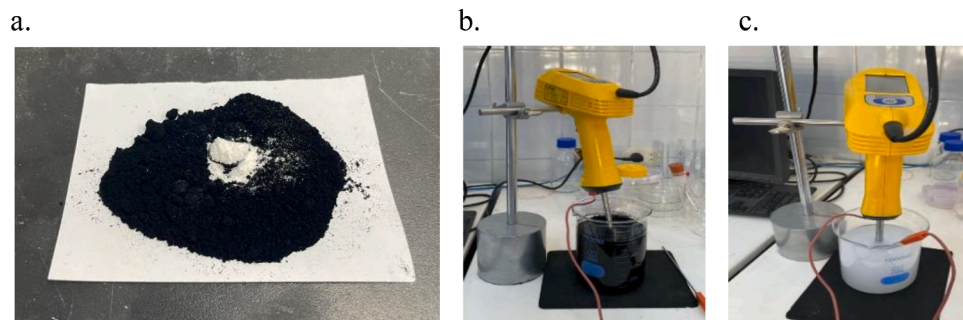


Fig. 5. a) Hybrid MWCNT/Al<sub>2</sub>O<sub>3</sub> nanoparticles b) MWCNT/water c) Al<sub>2</sub>O<sub>3</sub>/water nanofluids preparation

**Table 5**

The features of water and solid particles.

property	Symbol	Unit	Water	Al <sub>2</sub> O <sub>3</sub>	MWCNT
Density	$\rho$	(kg.m <sup>-3</sup> )	998.2	3970	2100
Specific Heat	$C_p$	(J.kg <sup>-1</sup> .k <sup>-1</sup> )	4182	765	519
Thermal Conductivity	$K$	(W.m <sup>-1</sup> .k <sup>-1</sup> )	0.6	40	3000
Viscosity	$\mu$	(kg. m <sup>-1</sup> .s <sup>-1</sup> )	0.001	—	—

create gamma alumina nanoparticles. TEM was carried out on a JEOL JEM-2100 high-resolution TEM at a 200 kV accelerating voltage. The TEM and XRD images for Al<sub>2</sub>O<sub>3</sub> and MWCNT nanoparticles are shown in Figs. 3 and 4, and the MWCNT and Al<sub>2</sub>O<sub>3</sub> particles' properties are shown in Tables 3 and 4.

Using an ultrasonic homogenizer (Sonicator), the nanoparticles were mixed with the distilled water to create the nanofluids, the Hielscher UP200HT. The homogenizer was utilized for 3 h at f of 50 Hz with a 100 percent amplitude and t of 20 s ON and 10 s OFF pulses until perfect dispersion was obtained. Fig. 5a. depicts hybrid Al<sub>2</sub>O<sub>3</sub>- MWCNT nanoparticles, whereas Figs. 5b. and c. depict the nanofluids' preparation. The MWCNT, Al<sub>2</sub>O<sub>3</sub>, and H<sub>2</sub>O features are shown in Table 5.

### 2.3. Mathematical calculations

Solar energy is a form of energy for harnessing solar energy to generate thermal energy for use in different with a weak effect on the environment.

The thermal energy-balanced equation for steady-state conditions [32] can be expressed as:

$$\dot{Q}_u = \dot{Q}_{Abs} - \dot{Q}_{loss} \quad (1)$$

Where,  $\dot{Q}_u$  is the useful gained energy from  $\dot{Q}_{Abs}$ ,

$\dot{Q}_{Abs}$  is the total amount of solar energy collected, excluding losses due to convection, conductivity, and irradiation between both the environment and the collector, and  $\dot{Q}_{loss}$  is the total lost energy between the collectors and the surrounding atmosphere and can be calculated by:

$$\dot{Q}_{loss} = U_L A_c (T_M - T_a) \quad (2)$$

Where  $U_L$  is the overall heat transfer coefficient,  $A_c$  is the area of the collector, and  $T_M$  and  $T_a$  are the mean plate temperature and the ambient temperature respectively.

$$\dot{Q}_u = \dot{m} C_p (T_o - T_i) \quad (3)$$

$T_o$  and  $T_i$  are the working fluid's output temperature and inlet temperature, respectively, while  $C_p$  is the heat capacity of the working fluid, which may be water or a nanofluid. The gained usable energy can be computed as:

$$\dot{Q}_u = A_c F_R [I_T (\tau\alpha) - U_L (T_i - T_o)] \quad (4)$$

Where, ( $F_R$ ) is the heat removal factor which refers to the ratio between the usable heat acquired and the energy obtained if the collector's interface temperature is the same as the inlet temperature, and  $I_T$  is the solar radiation.  $F_R$  can be calculated by the following equation [20,21]:

$$F_R = \frac{\dot{m} C_p (T_o - T_i)}{A_c [I_T (\tau\alpha) - U_L (T_i - T_a)]} \quad (5)$$

The Total Irradiation Received by the collector is calculated as:

$$q_{IT} = I_T A_c \quad (6)$$

Solar thermal efficiency refers to the ratio between the rates of useful heat ( $\dot{Q}_u$ ) transferred by solar radiation on the solar heater. The formula provided below can be used to calculate thermal efficiency [33].

**Table 6**

Uncertainty percentages of experimental measuring instruments.

Parameter	Uncertainty
H	5%
$\dot{m}$	±1.5%
T	±1.5%
$I_T$	±2%

$$\eta = \frac{\dot{Q}_u}{I_T A_c} = F_R \left[ (\tau\alpha) - U_L \frac{(T_i - T_a)}{I_T} \right] \quad (7)$$

The following equation can be used to compute the exergy efficiency [33], which is defined as the highest output a system can produce concerning the ambient temperature.

$$\eta_{ex} = 1 - T_a S_{gen} / [1 - (T_a / T_s)] q_{abs} \quad (8)$$

The base fluid and nanoparticles' thermal conductivities are combined to form the nanofluid thermal conductivity. The following adapted equations are used for the nanofluid properties calculation [34]

$$K_{nf} = (1 - \varphi) K_{bf} + \varphi K_{np} \beta \quad (9)$$

where  $K_{nf}$ ,  $K_{bf}$ , and  $K_s$  are the thermal conductivity for nanofluid, base fluid, and nanoparticles, respectively. The formula given by ( $\varphi$ ) gives the nanofluid volume concentration.:

$$\varphi = \frac{\frac{W_{nf}}{\rho_{nf}}}{\frac{W_{nf}}{\rho_{nf}} + \frac{W_{bf}}{\rho_{bf}}} \quad (10)$$

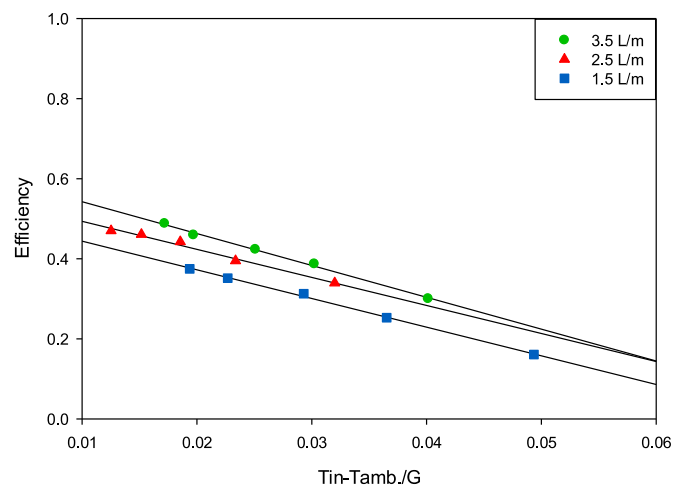
The specific heat and density of nanofluids can be represented by:

$$C_{pNF} = \frac{(1 - \varphi) \rho_{bf} C_{pbf} + \varphi \rho_s C_{ps}}{\rho_{nf}} \quad (11)$$

$$\rho_{nf} = \rho_{np} (\varphi) + \rho_{bf} (1 - \varphi) \quad (12)$$

### 2.4. Uncertainty analysis

A flawless measurement cannot be made, and the experimental measurements revealed some errors. The mistakes were caused by systemic flaws in calibration and data recording, as well as data variations caused by inappropriate instrumentation (random errors). To determine the divergence between the actual readings and the experimental data, the uncertainty of measurement outcomes was estimated. The experi-

**Fig. 6.** ETSC recorded efficiency at 1.5, 2.5, and 3.5 L/m of H<sub>2</sub>O.

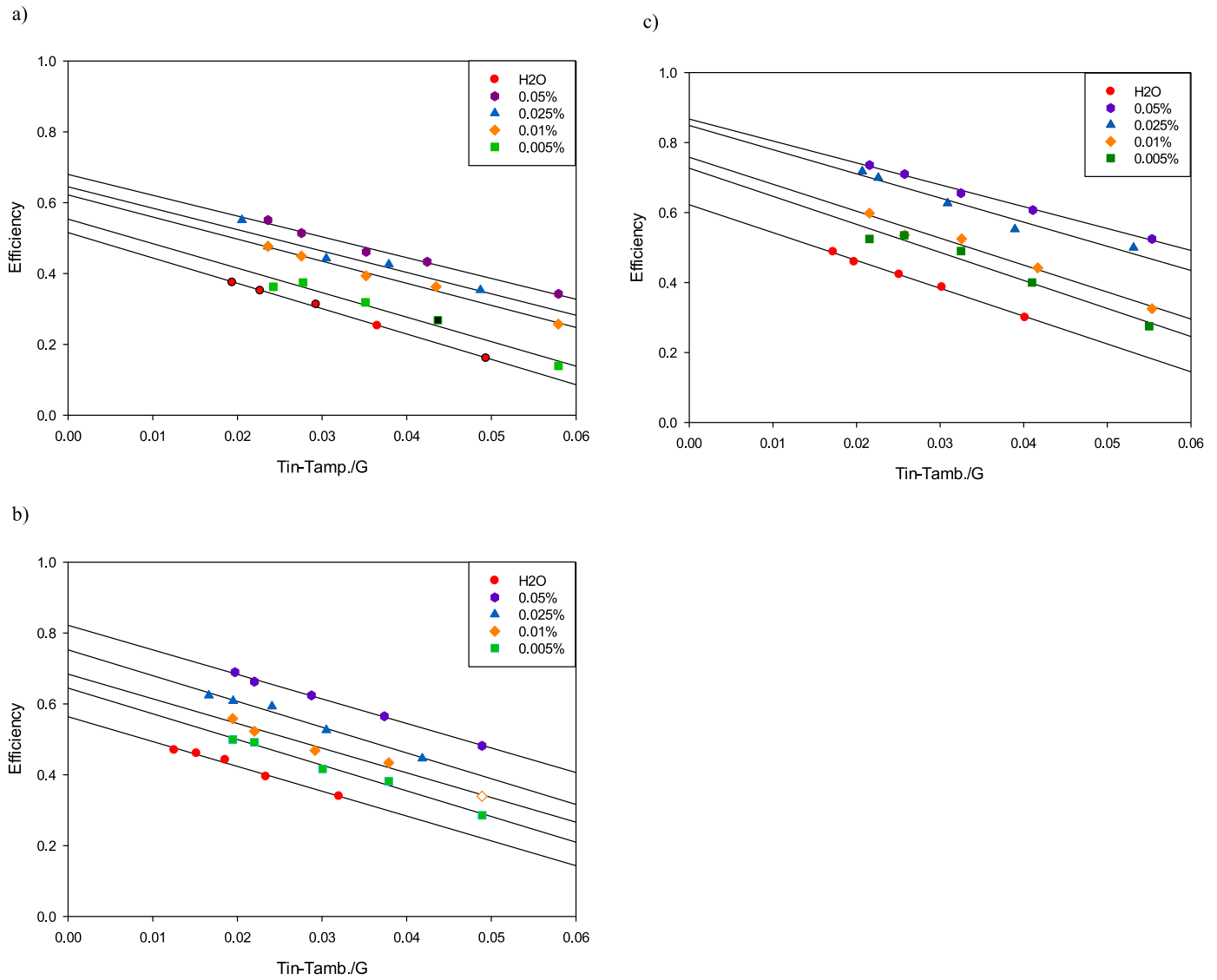


Fig. 7. ETSC efficiency for H<sub>2</sub>O, 0.05%, 0.025%, 0.01%, and 0.005% MWCNT at a) 1.5, b)2.5, and c) 3.5 L/m.

ment’s error assessment is a requirement for trust in the observed results. Analyses of uncertainty focus on test measurements, which are always associated with a range of uncertainty. The analytical equation for uncertainty has the general form shown below [35]:

$$U_y^2 = \sum_{x=1}^n U_{xi}^2 \tag{13}$$

The used standard equation for observing the uncertainty analysis of the applied system while ignoring C<sub>p</sub> and A<sub>c</sub> is as follows.:

$$U_y = \eta \times \sqrt{\left(\frac{\Delta \dot{m}}{\dot{m}}\right)^2 + \left(\frac{\Delta(T_o - T_i)}{(T_o - T_i)}\right)^2 + \left(\frac{\Delta G}{G}\right)^2} \tag{14}$$

Table 6 describes the features and accuracy of the sensors and monitoring equipment used in the current experimental setting.

### 3. Results and discussion

#### 3.1. Distilled water results

With [(T<sub>i</sub>-T<sub>a</sub>)/G] retained on the graph’s X-axis and the efficiency (η) on the Y-axis at three distinct flow rates 1.5, 2.5, and 3.5 L/min with a 5-minutes interval time, the experimental results are recorded and shown

based on the collector’s efficiency against the falling temperature variables for the ETSC as shown in Fig. 6. Tests had been carried out on the solar collector temperature outputs and the varying efficiency of the collector is mainly based on the base fluid flow rate according to the type of collector. The efficiency of the collectors was found to rise with higher fluid flow rates.

For the 1.5 L/m flow rate, the changes in the efficiency regarding (T<sub>i</sub>-T<sub>a</sub>)/G increased from 0.16 to 0.37 within the parameters of our investigation. Similar to this, the efficiency varied between 0.30 and 0.47 for the 2.5 L/m flow rate and from 0.34 to 0.48 for the 3.5 L/m flow rate. The F<sub>R</sub>U<sub>L</sub> recorded values were 3.27, 3.38, and 3.52, respectively, at each concentration, matching the slope of all linear methods. The efficiency decreased as the (T<sub>i</sub>-T<sub>a</sub>)/G increased, as was to be expected. For the flow rates of 1.5 L/m, 2.5 L/m, and 3.5 L/m, respectively, the average variances were 43.0 percent, 70 percent, and 72 percent. Also, increases in the decreased temperature parameter [(T<sub>i</sub>-T<sub>a</sub>)/G] result in greater inlet fluid temperatures, which raise the fluid’s bulk temperature and increase convection losses over the studied range. Changes in (T<sub>i</sub>-T<sub>a</sub>)/G have a significant impact on the heat transmission and circulation between the solar collector and the glazed covering, which has an important effect on the precision of the total heat transfer coefficient and the solar collectors’ thermal efficiency.

It was observed and shown how the mass flux rate of distilled water

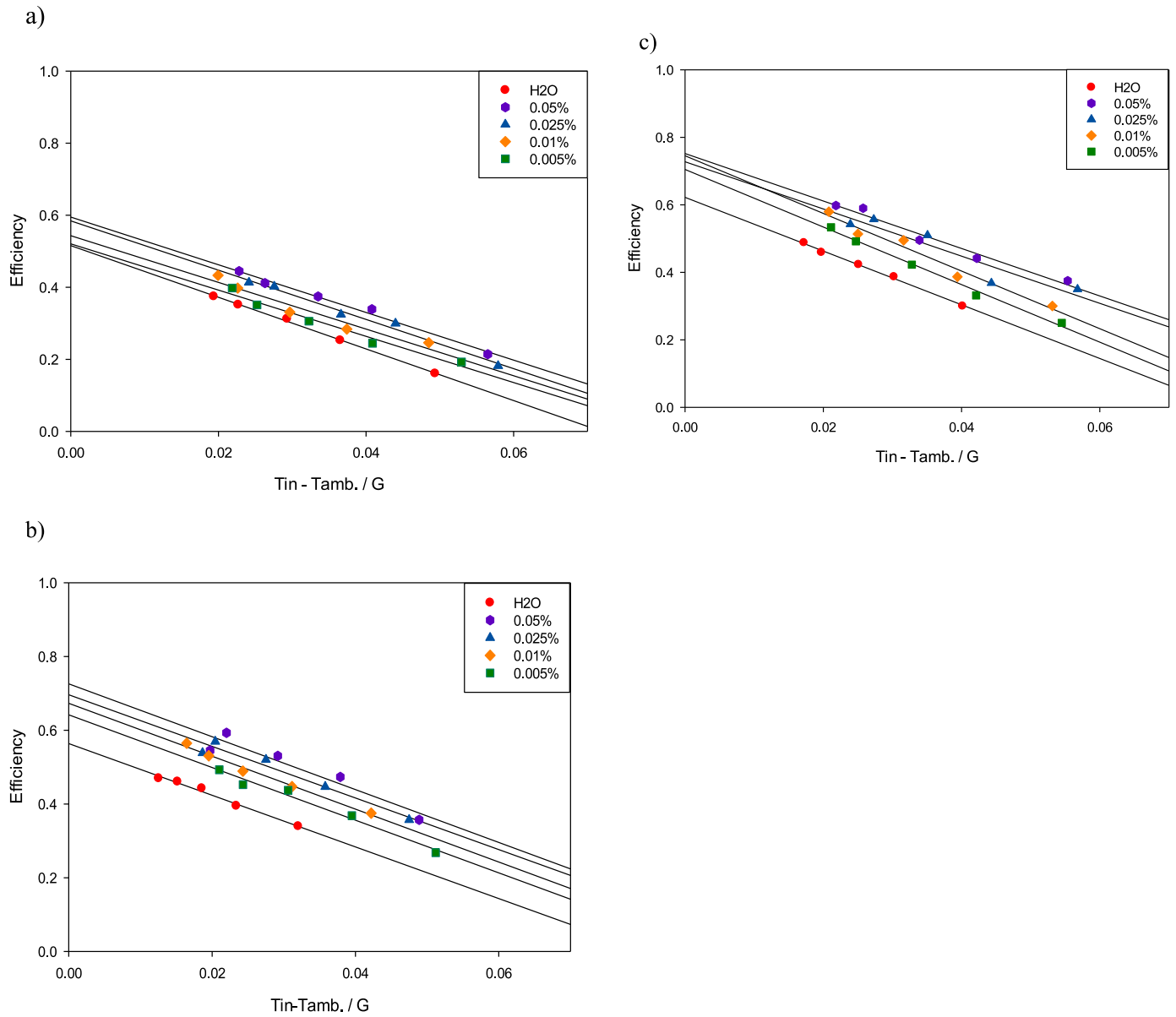


Fig. 8. ETSC efficiency for H<sub>2</sub>O, 0.05%, 0.025%, 0.01%, and 0.005% Al<sub>2</sub>O<sub>3</sub> at a) 1.5, b) 2.5, and c) 3.5 L/m.

affected the ETSC's efficiency. The comparison between the different water flow rates shown in Fig. 6 indicates that the higher flow rates have greater efficiency than lower flow rates for the same conditions, as a result of increasing the temperature difference between the receiver's exit and inlet, where turbulent flow is dominant.

### 3.2. MWCNT/ water results

Fig. 7 shows the results of testing four different MWCNT concentrations at three distinct mass flux rates for ETSC. The collector's efficiency can be improved by changing the nanofluid type, concentration, and mass flux rate. The Reynolds number rises as the mass flux rate rises, increasing the motion rate, and turbulence for the Brownian motion particles. The heat transfer rate is considerably affected by nanoparticle movement, which leads to an improvement in collector efficiency. In addition, the working fluid's thermal conductivity has a significant impact on the energy efficiency of solar collectors. As shown in Fig. 7, escalating the weighted fragment of MWCNT in the base fluid enhances the thermal conductivity of the fluid, which enhances the fluid's gains in heat. When employing nanofluids, combining both elements has a

twofold effect. For the four MWCNT concentrations, it can be seen that raising the mass flux rate enhances efficiency. At all mass flux rates, 0.05% wt. percent MWCNT/water achieves the maximum absorbed energy increase, as shown in the figure, the favorable effect of raising the mass flux rate, on the other hand, diminishes as the concentration rises.

The MWCNT concentrations 0.05%, 0.025%, 0.01%, and 0.005% by weight in the distilled water were used in this experiment. Initially, the system's effectiveness was determined by using a control fluid. On the X-axis of the graph, the temperature parameter ( $T_{in} - T_{amb.} / I_T$ ) was retained, while the efficiency ( $\eta$ ) was recorded on the Y-axis. Fig. 7 shows the efficiency of the ETSC at varied flow rates for the four given concentrations of MWCNT/water nanofluid. The average collector efficiencies for the varied concentrations of the MWCNT/water nanofluids were 57%, 54%, 44%, and 39%, respectively. The utilization of MWCNT/water nanofluid as the operating fluid enhanced the collector's efficiency, as seen in Fig. 7. The working fluid's thermal conductivity and absorption coefficient, as well as the heat transfer between the receiver and the coolant, were all improved by the nanostructures. adding a small concentration percentage of MWCNTs, the network efficiency increased significantly. The MWCNT nanofluid heat extraction



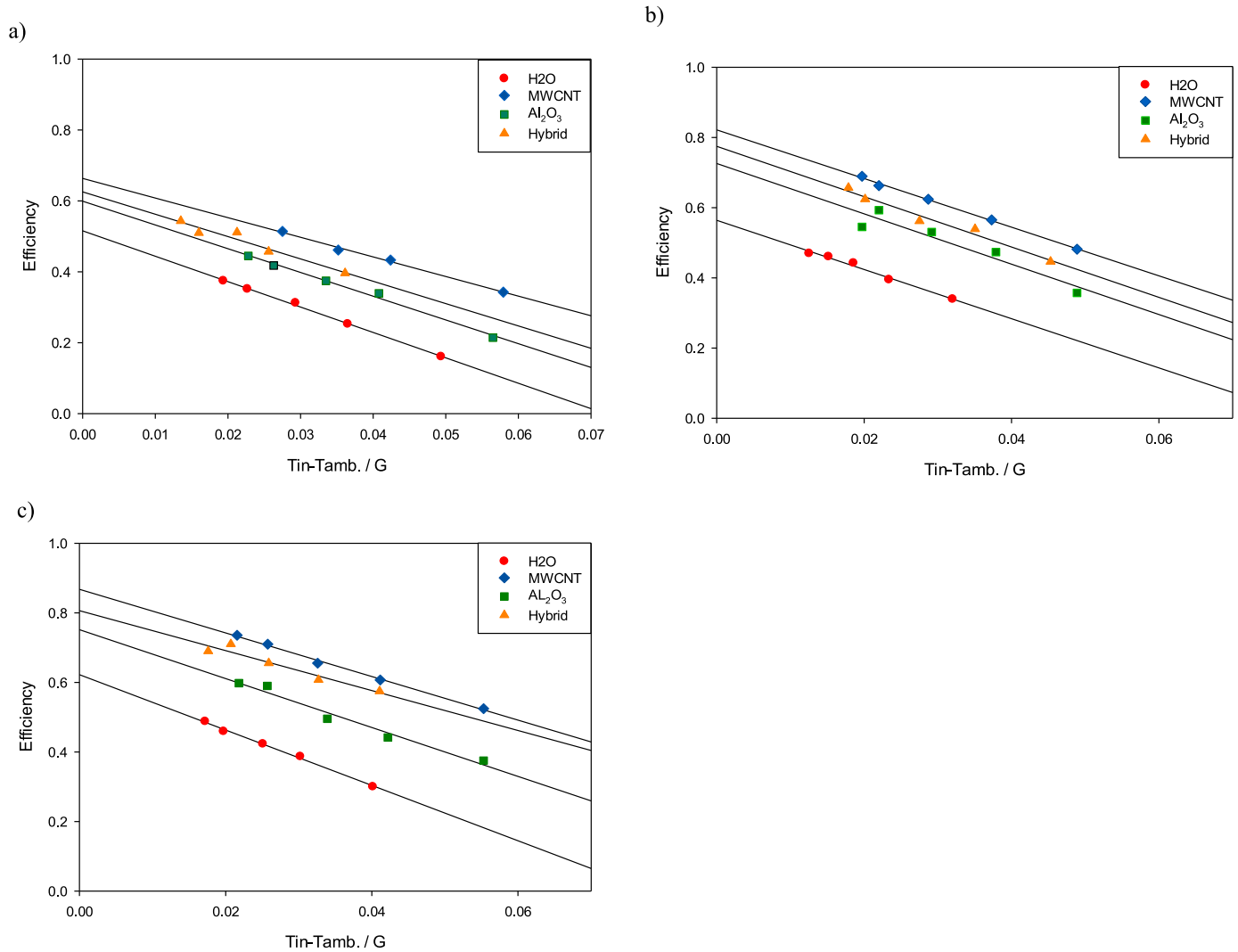


Fig. 9. ETSC efficiency at a)1.5, b)2.5, and c)3.5 L/m for 0.05% MWCNT, 0.05%Al<sub>2</sub>O<sub>3</sub>, and hybrid MWCNT/Al<sub>2</sub>O<sub>3</sub> 50:50%.

parameter of the absorber  $F_R$  was calculated for each weight percentage. The nanofluid's heat removal factor is higher than that of pure water, and it also increases when the weight percentage of MWCNTs increases and the received energy factor rises. When utilizing an MWCNT nanofluid, boosting these parameters enhances the effectiveness of the collector. Adding MWCNTs raised the absorbed energy parameter ( $F_R (\tau\alpha)$ ) of pure water by 23.6%, 31.2%, 40.5%, and 51.1% for nanoparticle concentrations of 0.005%, 0.01%, 0.025%, and 0.05% respectively.

### 3.3. Al<sub>2</sub>O<sub>3</sub>/ water results

As previously mentioned in the MWCNT/water investigation, similar concentrations of Al<sub>2</sub>O<sub>3</sub> were utilized to observe the enhancement in the solar collector's efficiency. Fig. 8 demonstrates the enhancement in the ETSC's efficiency with different concentrations and mass flow rates of Al<sub>2</sub>O<sub>3</sub>/water nanofluid. For the studied concentrations, the average collector effectiveness was 60%, 54%, 53%, and 50%, successively at 3.5 L/m. The figure illustrates how the efficiency trend has significantly improved on the plotted graph with the temperature parameter ( $T_{in} - T_{amb.} / G$ ) retained on X-axis, while the Y-axis represents the efficiency ( $\eta$ ) for ETSC, especially for higher flow rates.

It was determined that as flow rates are decreased, the amount of heat energy available decreases, the effectiveness of the nanoparticles decreases, and the influence of the nanoparticles on the temperature of the output fluid is less.

According to the findings, adding Al<sub>2</sub>O<sub>3</sub> nanoparticles to pure water improved the absorbent medium's ability to transfer heat. The graphs show that Al<sub>2</sub>O<sub>3</sub>/water with the four studied concentrations can enhance efficiency by 12%, 6%, 5%, and 2% respectively, compared to water at 3.5 L/m. Furthermore, the addition of Al<sub>2</sub>O<sub>3</sub> nanoparticles led to the decreased specific heat capacity of the fluid compared to plain base fluid; it requires lesser energy to reach higher temperatures which is the main target in the case of solar collectors. Finally, efficiency enhancement is lower in the case of Al<sub>2</sub>O<sub>3</sub> than in MWCNT because of its lower thermal conductivity.

### 3.4. Hybrid MWCNT/Al<sub>2</sub>O<sub>3</sub>/water 50:50%

Fig. 9 shows a graphical comparison of the prior findings utilizing nanofluid compositions of 0.025 wt percent MWCNTs and 0.025 wt percent Al<sub>2</sub>O<sub>3</sub>, with the hybrid form including 50:50 of each of the two materials. The hybrid MWCNT/ Al<sub>2</sub>O<sub>3</sub> (50:50%) is shown to give the average efficiency data staying between the two individual types. The hybrid material shows the average functionality of the hybrid nanofluid in the current study.

Results show that the use of hybrid nanofluid composed of 0.025 wt. % MWCNTs and 0.025 wt.% Al<sub>2</sub>O<sub>3</sub> resulted in approximately 20% enhancement in thermal efficiency at a flow rate of 3.5 L/min compared to distilled water. Graphs show that the enhancement in energy efficiency resulting from MWCNT/water is more than that of hybrid

**Table 7**  
Absorbed heat energy by ETSC for water and nanofluids at different concentrations.

Evacuated Tube Solar Collector					
Flow rate		Gained heat energy (W)		Gained heat energy (W)	Hybrid Fluid-Gained heat energy (W)
1.5	H <sub>2</sub> O	281.7247	H <sub>2</sub> O	281.7247	426.69
	MWCNT_0.05%	432.63	Al <sub>2</sub> O <sub>3</sub> _0.05%	341.3302	
	MWCNT_0.025%	421.2783	Al <sub>2</sub> O <sub>3</sub> _0.025%	313.7535	
	MWCNT_0.01%	368.732	Al <sub>2</sub> O <sub>3</sub> _0.01%	323.3908	
	MWCNT_0.005%	284.475	Al <sub>2</sub> O <sub>3</sub> _0.005%	288.6716	
2.5	H <sub>2</sub> O	390.5217	H <sub>2</sub> O	390.5217	527.162
	MWCNT_0.05%	562.0272	Al <sub>2</sub> O <sub>3</sub> _0.05%	467.4178	
	MWCNT_0.025%	518.3996	Al <sub>2</sub> O <sub>3</sub> _0.025%	455.0074	
	MWCNT_0.01%	437.6996	Al <sub>2</sub> O <sub>3</sub> _0.01%	449.9571	
	MWCNT_0.005%	393.7943	Al <sub>2</sub> O <sub>3</sub> _0.005%	383.2251	
3.5	H <sub>2</sub> O	386.7477	H <sub>2</sub> O	386.7477	593.05
	MWCNT_0.05%	600.1463	Al <sub>2</sub> O <sub>3</sub> _0.05%	472.4684	
	MWCNT_0.025%	578.3186	Al <sub>2</sub> O <sub>3</sub> _0.025%	440.3795	
	MWCNT_0.01%	457.8765	Al <sub>2</sub> O <sub>3</sub> _0.01%	435.6709	
	MWCNT_0.005%	440.6966	Al <sub>2</sub> O <sub>3</sub> _0.005%	393.8884	

**Table 8**  
Thermal efficiency comparison.

Author, Year	Investigation type, Conditions	Efficiency
Sabiha et al., 2015 [12]	Experimental, ETSC SWCNT/water 0.05% - 0.2%	48.57% - 93.43%
Mahbubul et al., 2018 [13]	Experimental, ETSC SWCNT/water 0.2 vol%	10% increase compared with water
Tong et al., 2015 [16]	Experimental, ETSC MWCNT/water 1%	The efficiency improved by 8% compared with that for water.
Kim et al., 2016 [17]	Theoretical, U-tube ETSC MWCNT/water 0.2 vol%	62.8%
Dehaj et al., 2019 [18]	Experimental, heat pipe ETSC MgO/water 0.014% - 0.032%	69% and 77% compared with 60% for water
Mahendran et al., 2012 [19]	Experimental, ETSC TiO <sub>2</sub> /water 2%	42.5% increase compared to water
Ghaderian and Sidik, 2017 [23]	Experimental, ETSC Al <sub>2</sub> O <sub>3</sub> /water 0.06%	36% enhancement, highest 58,65%
Eidan et al., 2018 [29]	Experimental, ETSC Al <sub>2</sub> O <sub>3</sub> and CuO/acetone 0.025% - 0.05%	34%, 74%, 32% and 73%, respectively
Shady M. Henein and Abdel-Rehim, 2022 [30]	Experimental, ETSC MWCNT/MgO/water 50:50% at 3 L/m	62%
	Experimental, ETSC MWCNT/water 0.05%, 0.025%, 0.01%, and 0.005% at 1.5, 2.5, and 3.5 L/m	55%, 53%, 47%, and 39% respectively at 1.5 L/m 69%, 62%, 55%, and 48% respectively at 2.5 L/m 73.5%, 71%, 59% and 52% respectively at 3.5 L/m
	Experimental, ETSC Al <sub>2</sub> O <sub>3</sub> /water 0.05%, 0.025%, 0.01%, and 0.005% at 1.5, 2.5, and 3.5 L/m	44%, 41%, 40%, and 38% respectively at 1.5 L/m 54%, 52%, 51%, and 46% respectively at 2.5 L/m 60%, 54%, 53% and 50% respectively at 3.5 L/m
	Experimental, ETSC MWCNT/ Al <sub>2</sub> O <sub>3</sub> /water 0.025% MWCNT/0.025% Al <sub>2</sub> O <sub>3</sub> /water at 1.5, 2.5, and 3.5 L/m	52% at 1.5 L/m 65% at 2.5 L/m 69% at 3.5 L/m

nanofluid by 3.5% while the hybrid nanofluid exceeds the Al<sub>2</sub>O<sub>3</sub>/water efficiency by 10% which reveals a great improvement in the system's total efficiency.

One of the main goals of this study is to compare the results of the utilized materials with other materials used as a nanofluid or hybrid nanofluid in ETSCs. Table 7 compares the energy efficiency outcomes of the experimental study with the outcomes of the earlier research described in the introduction section.

One of the most improved factors as a result of using nanofluids in ETSCs is the amount of gained heat energy. The given heat energy values for pure water compared with MWCNT/ Al<sub>2</sub>O<sub>3</sub> 50:50% in the ETSC are presented in Table 8. It shows an increase from a value of 281 W for the case of water to higher values of 432 W, 421 W, 368 W, and 284 W for the concentrations of 0.005, 0.01%, 0.025%, and 0.05%, respectively at a flow rate of 1.5 L/min. When the flow rate is increased to 2.5 L/min the gained energy is also enhanced to 562 W, 518 W, 437 W, and 393 W for 0.005, 0.01%, 0.025%, and 0.05%, respectively concerning 390 W for water. At the highest flow rates of 3.5 L/min, the supplied energy is discovered at its highest values, as their values are 600 W, 578 W, 457 W, and 440 W at 0.01%, 0.02%, and 0.03%, respectively, compared to 386 W for water.

Fig. 10 represents the useful heat gained for pure water compared with MWCNT and Al<sub>2</sub>O<sub>3</sub> in the ETSC. The useful heat gain can be expressed as the increasing percentage of the outlet temperature for the same mass flow rate. Using nanoparticles boosts the heat energy supplied by both systems, which is the main goal of this work. The thermal conductivity, heat capacity, and density of the solar collector's working fluids vary when nanoparticles are added. By intensifying heat transmission, increasing the thermal conductivity of the working fluid helps to increase the heat gain of the solar collector.

The heat removal factor (F<sub>R</sub>) is the proportion of the collector's actual usable heat energy transferred to the maximum available heat energy and is influenced by the fluid's thermos-physical properties; hence the addition of nanoparticles can enhance it. When the inlet fluid temperature is identical to the ambient temperature, the maximum amount of heat energy may be transported; no heat is lost to the surroundings. Also, because it appears at two parameters in the same equation, the heat removal factor F<sub>R</sub> has a double side effect on the collector's efficiency: absorbed energy parameter F<sub>R</sub>(τ<sub>α</sub>) and removal energy parameter F<sub>R</sub>U<sub>L</sub>. If the F<sub>R</sub> value rises, it signifies that more heat energy was absorbed, and the temperature of the outflow fluid increased. Also, as the temperature of the output fluid rises, the temperature of the collector's absorber plate rises, increasing heat loss with the ambient temperature.

To determine the maximum available energy that may be converted to usable heat, it is also necessary to study the exergetic efficiency of the ETSC. The exergy efficiency of solar systems refers to the exergy flow of the generated usable heat to the incident solar irradiation flow. Exergy analysis is a thermodynamic tool used to assess each energy source based on its properties, most commonly on its temperature levels. The exergy analysis is also used as an indicator to characterize and examine the investment opportunities of sustainable and green technology as well as renewable energy sources. Exergy helps in improving inefficiencies and reducing thermodynamic drops, which are in line with more environmentally friendly energy systems. Furthermore, it can aid in understanding the environmental and financial advantages of energy systems more precisely than energy analysis. By reducing energy losses, improving energy efficiency can lessen its negative effects on the environment.

Prepared nanofluids were tested at mass flow rates of 1.5, 2.5, and 3.5 L/m, with an exergy efficiency of 0.05 wt.% MWCNT, 0.05 wt.% Al<sub>2</sub>O<sub>3</sub>, and the hybrid MWCNT/ Al<sub>2</sub>O<sub>3</sub> (50:50%) nanofluids were determined. The addition of nanoparticles and an increase in mass flow rate improved the exergy efficiency. as shown in Fig. 11. For the same flow rate used in ETSC, the highest enhancement of the exergy efficiency is 51%, 44%, and 38% for MWCNT/water nanofluid, hybrid MWCNT/

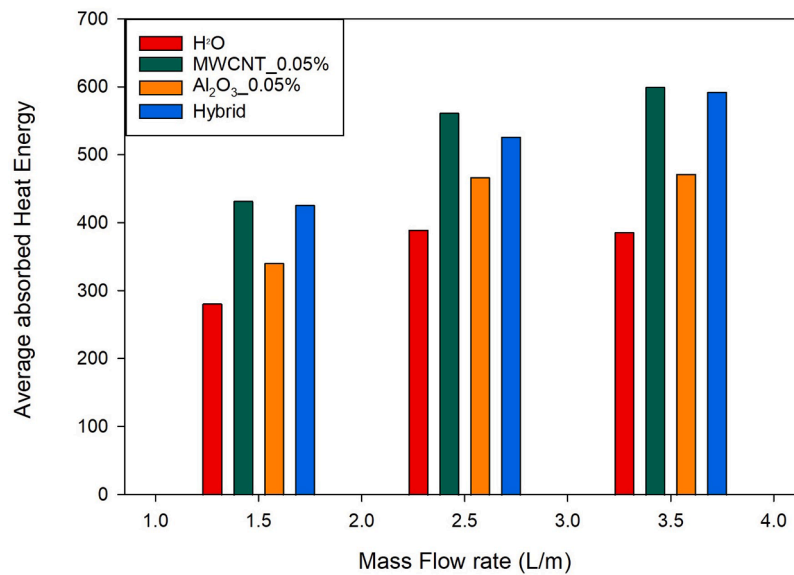


Fig. 10. Variation of the ETSC average absorbed heat energy at 1.5 L/m, 2.5 L/m, 3.5 L/m for water, 0.05%MWCNT, 0.05%Al<sub>2</sub>O<sub>3</sub>, hybrid MWCNT/ Al<sub>2</sub>O<sub>3</sub> 50:50%.

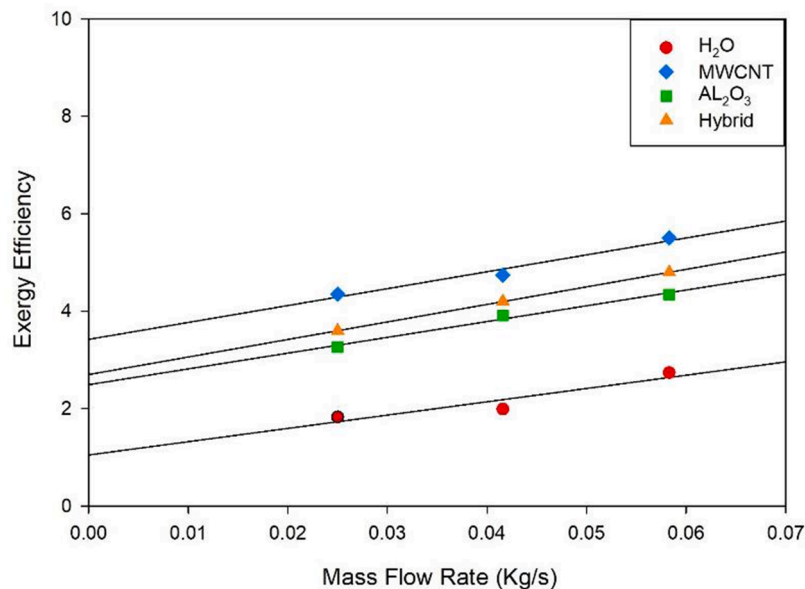


Fig. 11. ETSC exergy efficiency at different mass flow rates.

Al<sub>2</sub>O<sub>3</sub> (50:50), and Al<sub>2</sub>O<sub>3</sub> /water nanofluid compared to water, respectively. It can be concluded that hybrid nanofluid has improved the exergy efficiency higher than the Al<sub>2</sub>O<sub>3</sub> /water nanofluid but, still less than the MWCNT/water nanofluid.

The study employed different types of nanofluids for enhancing the thermal performance of solar collectors. The employed fluids included MWCNT, Al<sub>2</sub>O<sub>3</sub>, and the hybrid MWCNT/ Al<sub>2</sub>O<sub>3</sub> 50:50%. The general trend in the experiment was increasing efficiencies with increasing concentrations of the nanofluids. Also, the efficiency was directly affected by the flow rate of the fluids. Given in Fig. 12, the 3D surfaces illustrate the general trend of efficiencies with the two studied parameters; concentration and flow rate, which indicates the effect of high flow rate and concentration on the total efficiency for MWCNT and Al<sub>2</sub>O<sub>3</sub>. The MWCNT samples generated better efficiency results for all three composite fluids used in the experiments.

#### 4. Collector size reduction

Utilizing solar collectors primarily aims to increase the effective output of these collectors while lowering the cost of production. Fig. 13 shows a comparison between the reduced percentage in ETSC for the three studied nanomaterials.

The use of nanofluids as a working fluid can improve energy production and reduce the amount of used glass and copper used in the manufacturing process of solar collectors in addition to lowering emissions into the environment. It is concluded from Figs. 12 and 13 that the collector's efficiency and size reduction percentage are highly influenced by main three factors which are the used material, the flow rate, and the concentration of the used nanoparticles in the working fluid.

The highest size reduction percentage was 27% reported for MWCNT/water at 3.5 L/m compared to 25% for hybrid nanofluid, and 22% for Al<sub>2</sub>O<sub>3</sub>. These results reveal that using MWCNT/AL<sub>2</sub>O<sub>3</sub>/water 50:50% is highly recommended in ETSCs for the system's efficiency

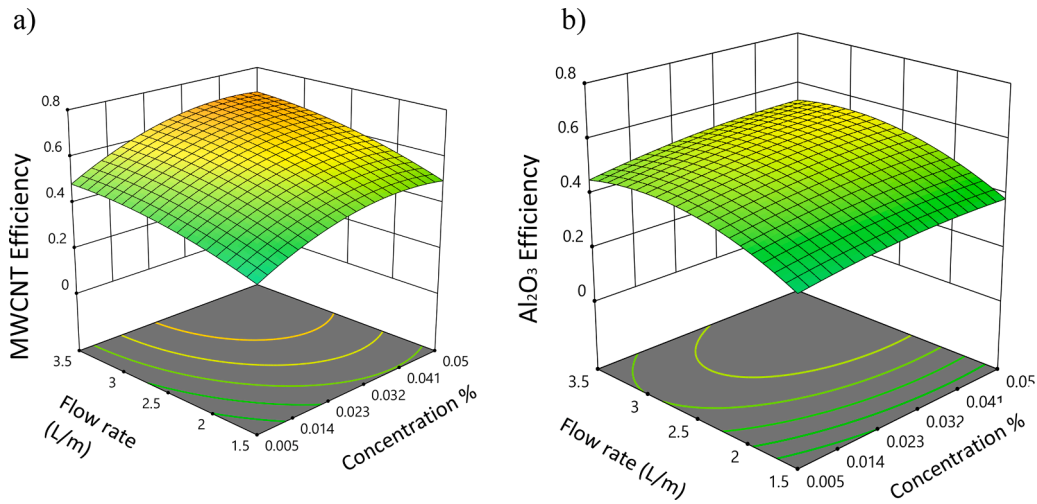


Fig. 12. 3D Illustration for flow rate and radiation effect of a) MWCNT and b) Al<sub>2</sub>O<sub>3</sub> on the ETSC efficiency.

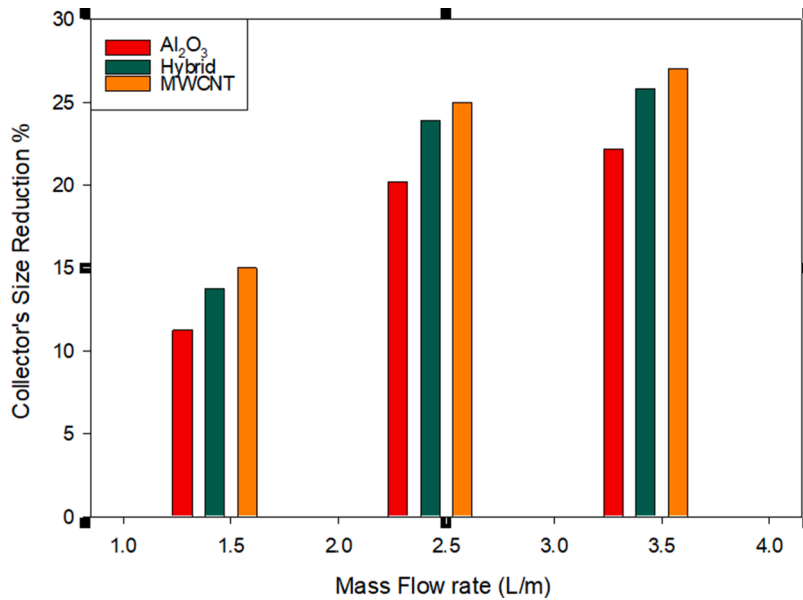


Fig. 13. ETSC size reduction percentage for 0.05% MWCNT, 0.05%Al<sub>2</sub>O<sub>3</sub>, and hybrid MWCNT/Al<sub>2</sub>O<sub>3</sub> 50:50%.

enhancement and cost reduction improvement.

### 5. Conclusion and future work

An experimental study was performed on a variety of nanofluids to improve the thermal performance of Evacuated Tube Solar Collectors. MWCNT, Al<sub>2</sub>O<sub>3</sub>, and a hybrid MWCNT/ Al<sub>2</sub>O<sub>3</sub> (50:50 percent) were examined. The basic finding is that

- The concentration of nanoparticles and the fluid flow velocity have a direct impact on ETSC efficiency.
- For all three composite fluids utilized in the trials, the MWCNT has the highest efficiency.
- The average efficiency of MWCNT was approximately 8% greater than Al<sub>2</sub>O<sub>3</sub> under the same experimental conditions.
- This research indicates that replacing half of the Al<sub>2</sub>O<sub>3</sub> with MWCNTs (50:50) increases efficiency by an average of 20% compared to that reported for Al<sub>2</sub>O<sub>3</sub>, and this percentage is affected significantly by increasing the fluid’s mass flow rate, recommending

that 50% of the MWCNTs can be replaced with the more cost-effective and eco-friendlier Al<sub>2</sub>O<sub>3</sub>.

- It is recommended to study the impact of different volume fractions of MWCNT/ Al<sub>2</sub>O<sub>3</sub> and study the rheological behavior of nanofluids. In addition, there is a need to emphasize the stability of different nanofluids.

### Declaration of Competing Interest

The authors declare the following financial interests/personal relationships which may be considered as potential competing interests: Engy Elshazly reports equipment, drugs, or supplies was provided by The British University in Egypt. Engy Elshazly reports a relationship with The British University in Egypt that includes: employment.

### Data availability

Data will be made available on request.



## Acknowledgements

The authors are extremely grateful to the Centre of Renewable Energy (CRE) at the British University in Egypt for providing the experimental apparatus and equipment to carry out the research.

## References

- [1] S.U. Choi, J.A. Eastman, Enhancing Thermal Conductivity of Fluids With Nanoparticles (No. ANL/MSD/CP-84938; CONF-951135-29), Argonne National Lab., IL (United States), 1995.
- [2] M.M.A. Khan, N.I. Ibrahim, I.M. Mahbulul, H.M. Ali, R. Saidur, F.A. Al-Sulaiman, Evaluation of solar collector designs with integrated latent heat thermal energy storage: a review, *Sol. Energy* 166 (2018) 334–350, <https://doi.org/10.1016/j.solener.2018.03.014>.
- [3] Y. Khanjari, F. Pourfayaz, A.B. Kasaean, Numerical investigation on using of nanofluid in a water-cooled photovoltaic thermal system, *Energy Convers. Manag.* 122 (2016) 263–278, <https://doi.org/10.1016/j.enconman.2016.05.083>.
- [4] F. Kiliç, T. Menlik, A. Sözen, Effect of titanium dioxide/water nanofluid use on thermal performance of the flat plate solar collector, *Sol. Energy* 164 (2018) 101–108, <https://doi.org/10.1016/j.solener.2018.02.002>.
- [5] Hamza Babar, Hafiz Muhammad Ali, Towards hybrid nanofluids: preparation, thermophysical properties, applications, and challenges, *J. Mol. Liq.* 281 (2019) 598–633.
- [6] M. Awais, N. Ullah, J. Ahmad, F. Sikandar, M.M. Ehsan, S. Salehin, A.A. Bhuiyan, International Journal of Thermo fluids Heat transfer and pressure drop performance of Nanofluid : a state-of-the-art review, *Int. J. Thermofluids* 9 (2021), 100065, <https://doi.org/10.1016/j.ijft.2021.100065>.
- [7] D. Wen, G. Lin, S. Vafaei, K. Zhang, Review of nanofluids for heat transfer applications, *Particuology* 7 (2) (2009) 141–150.
- [8] M. Yahya, M.Z. Saghir, Thermal analysis of flow in a porous flat tube in the presence of a nanofluid: numerical approach, *Int. J. Thermofluids* 10 (2021) 100095.
- [9] A.H. Elsheikh, S.W. Sharshir, M.E. Mostafa, F.A. Essa, M.K.A. Ali, Applications of nanofluids in solar energy: a review of recent advances, *Renew. Sustain. Energy Rev.* 82 (2018) 3483–3502.
- [10] W.S. Sarsam, S.N. Kazi, A. Badarudin, A review of studies on using nanofluids in flat-plate solar collectors, *Sol. Energy* 122 (2015) 1245–1265.
- [11] F.P. Incropera, T.L. Bergman, A.S. Lavine, D.P. DeWitt, Fundamentals of, heat mass transf. <https://doi.org/10.1073/pnas.0703993104>. 2011.
- [12] M.A. Sabiha, R. Saidur, S. Mekhilef, An experimental study on evacuated tube solar collector using nanofluids, *Trans. Sci. Technol.* 2 (1) (2015) 42–49.
- [13] I. Mahbulul, M.M.A. Khan, N.I. Ibrahim, H.M. Ali, F.A. Al-Sulaiman, R. Saidur, Carbon nanotube nanofluid in enhancing the efficiency of evacuated tube solar collector, *Renew. Energy* 121 (2018) 36–44.
- [14] ... Z. S. R. S. M. S. N. R. M. A. Thermophysical properties of single wall carbon nanotubes and its effect on exergy efficiency of a flat plate solar collector *Sol. Energy* 115 (2015) 757–769.
- [15] .. M. F. R. S. S. Mekhilef, Potential of size reduction of flat-plate solar collectors when applying MWCNT nanofluid, in: Proceedings of the 4th International Conference on Energy and Environment (ICEE 2013), 2013, pp. 1–4.
- [16] T. Yijie, K. Jinhyun, C. Honghyun, Effects of thermal performance of enclosed-type evacuated U-tube solar collector with multi-walled carbon nanotube/water nanofluid, *Renew. Energy* 83 (2015) 463–473.
- [17] H. Kim, J. Ham, C. Park, H. Cho, Theoretical investigation of the efficiency of a U-tube solar collector using various nanofluids, *Energy* 94 (2016) 497–507.
- [18] M.S. Dehaj, M.Z. Mohiabadi, Experimental investigation of heat pipe solar collector using MgO nanofluids, *Sol. Energy Mater. Sol. Cells* 191 (2019) 91–99.
- [19] M. Mahendran, G.C. Lee, K.V. Sharma, A. Shahrani, Performance evaluation of evacuated tube solar collector using water-based titanium oxide (TiO<sub>2</sub>) nanofluid, *J. Mech. Eng. Sci.* 3 (2012) 301–310.
- [20] B. Farajollahi, S.G. Etamad, M. Hojjat, Heat transfer of nanofluids in a shell and tube heat exchanger, *Int. J. Heat Mass Transf.* 53 (2010) 12–17.
- [21] W. He, D. Toghraie, A. Lotfipour, F. Pourfatah, A. Karimipour, M. Afrand, Effect of twisted-tape inserts and nanofluid on flow field and heat transfer characteristics in a tube, *Int. Commun. Heat Mass* 110 (2020), 104440, <https://doi.org/10.1016/j.icheatmasstransfer.2019.104440>.
- [22] N.S. Rajput, D.D. Shukla, D. Rajput, S.K. Sharm, Performance analysis of flat plate solar collector using Al<sub>2</sub>O<sub>3</sub>/distilled water nanofluid: an experimental investigation, *Mater. Today: Proc.* 10 (2019) 52–59, <https://doi.org/10.1016/j.matpr.2019.02.1882019>.
- [23] J. Ghaderian, N.A.C. Sidik, An experimental investigation on the effect of Al<sub>2</sub>O<sub>3</sub>/distilled water nanofluid on the energy efficiency of evacuated tube solar collector, *Int. J. Heat Mass Transf.* 108 (2017) 972–987.
- [24] A. Mahamude, M. Kamarulzaman, W. Harun, K. Kadirgama, D. Ramasamy, K. Farhana, et al., A comprehensive review on efficiency enhancement of solar collectors using hybrid nanofluids, *Energies* 15 (4) (2022) 1391, <https://doi.org/10.3390/en15041391>.
- [25] Shu-Rong Yana, Davood Toghraie, Lokman Aziz Abdulkareem, As'ad Alizadehd, Pouya Barnoon, Masoud Afrand, The rheological behavior of MWCNTs–ZnO/water–ethylene glycol hybrid non-Newtonian nanofluid by using of an experimental investigation, *J. Mater. Res. Technol.* 9 (4) (2020) 8401–8406. July–August 2020.
- [26] Pouya Barnoon, Numerical assessment of heat transfer and mixing quality of a hybrid nanofluid in a microchannel equipped with a dual mixer, *Int. J. Thermofluids* 12 (2021), 100111. November 2021.
- [27] Behrooz Ruhani, Davood Toghraie, Maboud Hekmatifar, Mahdieh Hadian, 2019. Statistical investigation for developing a new model for rheological behavior of ZnO–Ag (50%–50%)/water hybrid Newtonian nanofluid using experimental data", Volume 525, 1 July 2019, Pages 741–75.
- [28] S.S. Harandi, A. Karimipour, M. Afrand, M. Akbari, A.J. D'Orazio, An experimental study on thermal conductivity of FMWCNTs–Fe<sub>3</sub>O<sub>4</sub>/EG hybrid nanofluid: effects of temperature and concentration, *Int. Commun. Heat Mass Transf.* 76 (2016) 171–177.
- [29] A.A. Eidan, A. AlSahlani, A.Q. Ahmed, M. Al-fahham, J.M. Jalil, Improving the performance of heat pipe-evacuated tube solar collector experimentally by using Al<sub>2</sub>O<sub>3</sub> and CuO/acetone nanofluids, *Sol. Energy* 173 (2018) 780–788.
- [30] M.Henein Shady, A.Abdel-Rehim Ahmed, The performance response of a heat pipe evacuated tube solar collector using MgO/MWCNT hybrid nanofluid as a working fluid, *Case Stud. Therm. Eng.* 33 (2022) (2022), 101957.
- [31] Babar Hamza, Ali Hafiz Muhammad, Towards hybrid nanofluids: preparation, thermophysical properties, applications, and challenges, *J. Mol. Liq.* 281 (2019) 598–633.
- [32] S. Gorjian, H. Ebadi, F. Calise, A. Shukla, C. Ingraio, A review on recent advancements in performance enhancement techniques for low-temperature solar collectors, *Energy Convers. Manag.* 222 (2020), 113246.
- [33] Muhammad Abid, Muhammad Sajid Khan, Tahir Abdul Hussain Ratlamwala, Muhammad Nauman Malik, Hafiz Muhammad Ali, Quentin Cheok, Thermodynamic analysis and comparison of different absorption cycles driven by evacuated tube solar collector utilizing hybrid nanofluids, *Energy Conversion and Manag.* 246 (2021), 114673. ISSN 0196-8904.
- [34] M.S. Khan, M. Abid, M.i. Yan, T.A.H. Ratlamwala, I. Mubeen, Thermal and thermodynamic comparison of smooth and convergent-divergent parabolic trough absorber tubes with the application of mono and hybrid nanofluids, *Int. J. Energy Res.* 45 (3) (2021) 4543–4564.
- [35] R.J. Moffat, Using uncertainty analysis in the planning of an experiment, *J. Fluids Eng. Trans. ASME* 107 (2) (1985) 173–178, <https://doi.org/10.1115/1.3242452>.